Journal of Photochemistry and Photobiology A: Chemistry 200 (2008) 334–345

Contents lists available at ScienceDirect

Journal of Photochemistry and Photobiology A: Chemistry

journal homepage: www.elsevier.com/locate/jphotochem

Highly soluble perylene tetracarboxylic diimides and tetrathiafulvalene–perylene tetracarboxylic diimide–tetrathiafulvalene triads

Yu Zhang[a], Zheng Xu[b], Liangzhen Cai[c], Guoqiao Lai[b], Haixiao Qiu[a], Yongjia Shen[a,*]

[a] Lab for Advanced Materials and Institute of Fine Chemicals, East China University of Science and Technology, Shanghai 200237, PR China
[b] Key Lab of Organosilicon Chemistry and Material Technology of Ministry of Education, Hangzhou Normal University, Hangzhou 310012, PR China
[c] Department of Chemistry, East China University of Science and Technology, Shanghai 200237, PR China

ARTICLE INFO

Article history:
Received 24 April 2008
Received in revised form 19 July 2008
Accepted 16 August 2008
Available online 29 August 2008

Keywords:
Donor
Acceptor
Tetrathiafulvalene
Perylene tetracarboxylic diimide
Photoinduced electron transfer

ABSTRACT

Two donor-σ-acceptor-σ-donor triads incorporating tetrathiafulvalene (TTF) and 3,4,9,10-perylene tetracarboxylic diimides (PDI) units were synthesized. The structures of the triads and their intermediates were characterized by ^{1}H NMR, ^{13}C NMR, MS, IR. The results of UV–vis and cyclic voltammetry (CV) of the triads indicated negligible intramolecular charge transfer (ICT) interaction in their ground states. The fluorescence and fluorescence lifetimes of the triads were reduced compared to PDIs, which evidently indicated that photoinduced electron transfer (PET) interaction occurred from the TTF unit to the PDI unit in the excited state. The fluorescence intensity of the triads could be reversibly modulated by sequential oxidation and reduction of the TTF unit using the chemical methods. Therefore two new fluorescence molecular switches based on TTF and PDI units were established.

1. Introduction

Derivatives of perylene such as perylene diimides (PDI) have been widely employed and extensively studied in these molecular systems due to their high molar absorptivity, high quantum yields of fluorescence with excellent photochemical and thermal stabilities as well as electrochemical performance [1–8]. However, the poor solubility and difficult separation make the manufacture of this kind of wonderful dyes in material science confined.

Two methods are offered to increase the solubility of PDIs in organic solvents: (1) *N*-substituent in the "imide" region of PDIs, usually the long alkyl substitutions, to obtain the long-tail or swallow-tail conformation [9–11], however, this only enhances the solubility in a slight degree; (2) bis-substituent or tetra-substituent in the "bay" region of PDIs, to afford PDI dyes with the markedly improved solubility [12], 1,6,7,12-tetrachloro-3,4,9,10-perylene tetracarboxylic dianhydride (PDA) **1** (Fig. 1) is of importance among perylene derivatives [13–15]. We chose this perylene derivative to synthesize a series of PDI derivatives with tetrasubstituted *p*-*t*-butylphenoxy at the "bay" region and bis-*N*-substituent in the "imide" region (Fig. 1, Schemes 1 and 2), all these dyes have good solubility and outstanding chemical, thermal and photochemical stability.

The electrochemical properties of perylene diimides make them become the important electron acceptor and electron-transporting materials [16,17]. Specially remarkable for the construction of donor–acceptor (D–A) systems showing electron transfer are its good electron accepting ability [18]. Thus, PDIs have been recently linked to aligothiophenes [19], porphyrins[20], phthalocyanines [21] and tetraphenylbenzidines [22] as the counterpart aiming the induction of electron transfer. On the other hand, tetrathiafulvalene (TTF), such as TTF **7** (Fig. 1), has also been widely used to construct D–A molecular systems [23–31]. The possibility of exploiting the multistage redox state (TTF^{0}, $TTF^{\bullet+}$, TTF^{2+}) was investigated to construct molecular systems that can be controlled by external stimuli, such as TTF-based fluorescence-redox switches [32]. Researchers have tried to merge the perylene and TTF, however, to our knowledge, very few of this kind of donor–acceptor molecules had been achieved [32,33]. Thus, we are interested in the synthesis of triad **1** with a shorter chain between perylene and TTF units, and triad **2** with the aryl substitutions as the bridge of the donors and acceptors consisted of the highly soluble PDIs (Fig. 2). Herein, we report the synthesis (Schemes 3 and 4), spectroscopic and electrochemical properties of triad **1** and **2** together with their chemical redox performances. These two triads could finally act as the potential reversibly fluorescence-redox dependent molecular systems whose fluorescence intensity could be modulated by the oxidation state of TTF.

* Corresponding author. Tel.: +86 21 64252967; fax: +86 21 64252967.
E-mail address: yjshen@ecust.edu.cn (Y. Shen).

1010-6030/$ – see front matter © 2008 Elsevier B.V. All rights reserved.
doi:10.1016/j.jphotochem.2008.08.011

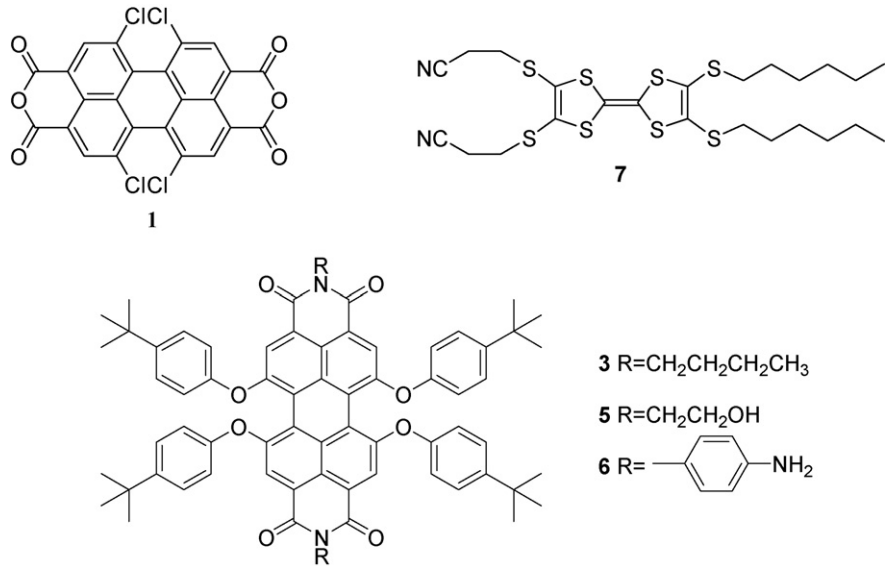

Fig. 1. The structures of PDA **1**, PDI **3**, **5**, **6** and TTF-bis-CH_2CH_2CN **7**.

2. Experimental

2.1. Chemicals and instruments

All chemicals were purchased commercially, PDI **2–4** were synthesized according to the literature [34,35], TTF **7**, **8** was synthesized according to the reported procedures [36–38] and the solvents dried or distilled when necessary using standard procedures. ^{1}H NMR and ^{13}C NMR were obtained on a Bruker AVANCE 500 spectrometer operating at 500 MHz and 100 MHz: chemical shifts were quoted downfield of TMS. Elemental analyses were obtained from a Elementar vario ELIII C, H, N analyzer. Infrared spectra were obtained on a NICOLET 5 SXC spectrometer. UV–vis spectra were recorded on a CARY 100 Conc UV–visible Spectrophotometer. The fluorescence spectra were recorded on a CARY Eclipse Fluorescence spectrophotometer and were corrected for the spectral response of the machines. The fluorescence lifetime experiment was performed on Edinburgh steady state and

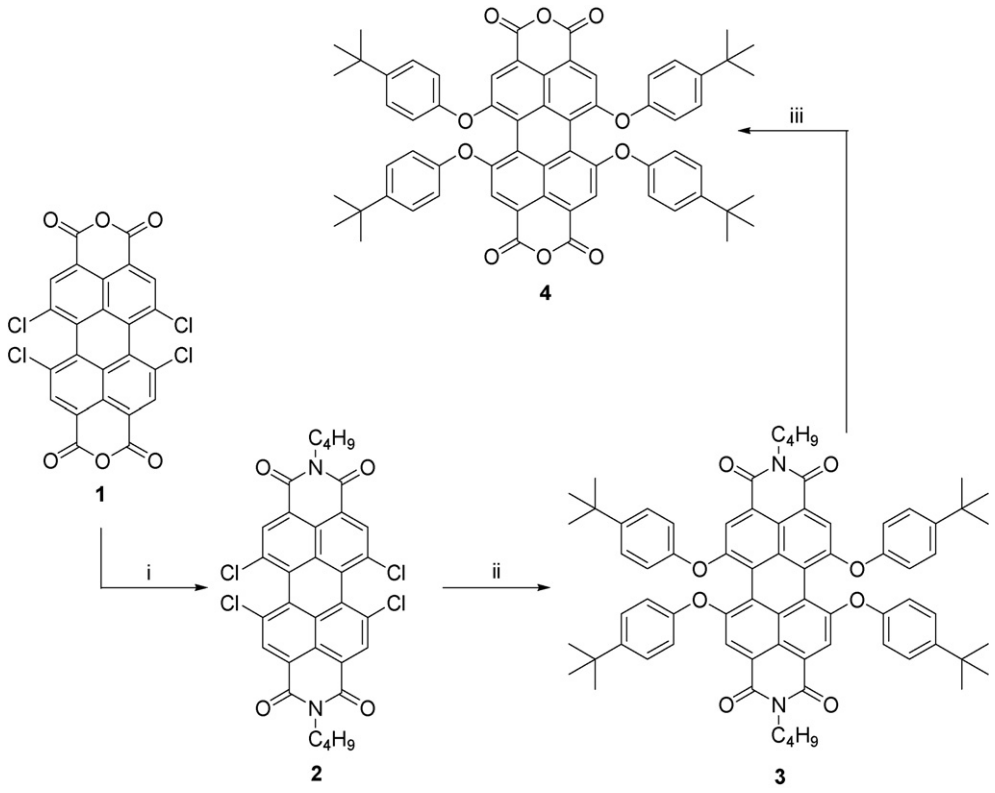

Scheme 1. Reagents and conditions: (i) $NH_2CH_2CH_2CH_2CH_3$, ethanol:H_2O = 1:1, reflux, 15 h, 92%; (ii) 4-*tert*-butylphenol, K_2CO_3, NMP, 180–190 °C, under N_2 atmosphere, 20 h, 75%; (iii) KOH, *t*-butanol, reflux, under N_2 atmosphere, 25 h, 68%.

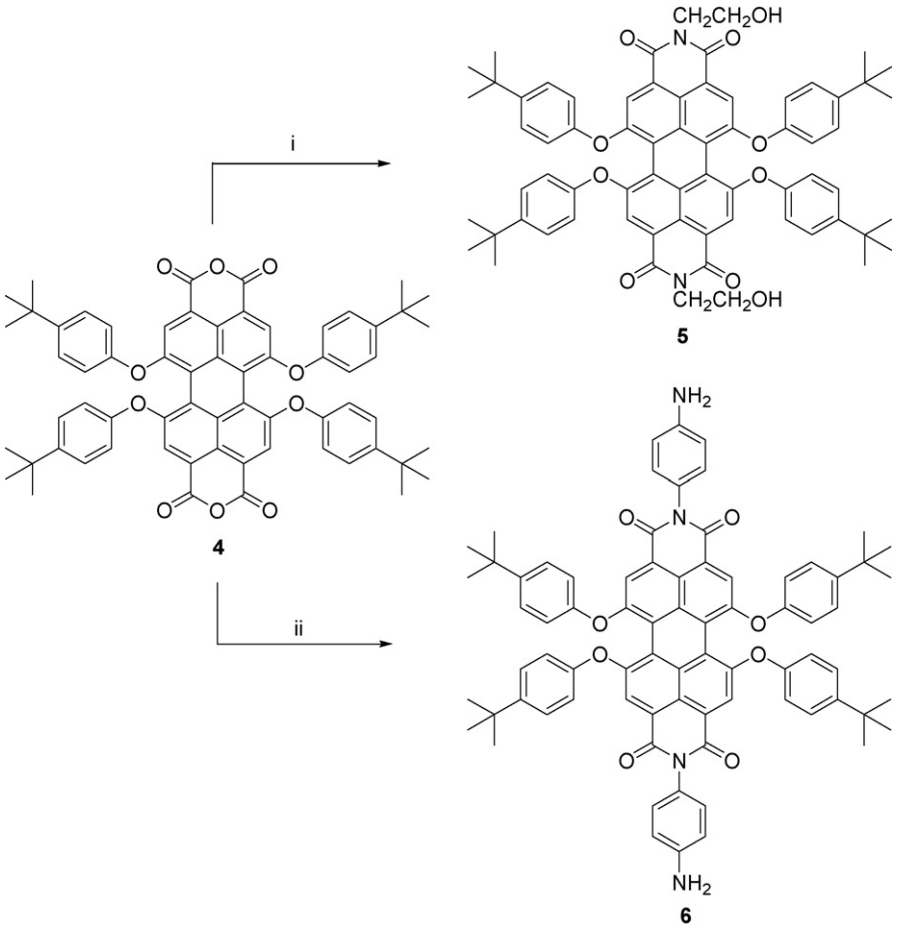

Scheme 2. Reagents and conditions: (i) 2-aminoethanol, toluene, reflux, 20 h, under N_2 atmosphere, 75%; (ii) *p*-phenylenediamime, pyridine, imidazole, reflux, 15 h, under N_2 atmosphere, 68%.

time resolved fluorescence spectrometers FL 900. Thermal gravimetric analysis experiments were performed on PerkinElmer 7 series thermal analysis system. All the electrochemical experiments were performed in dichloromethane with n-Bu_4NPF_6 as the supporting electrolyte, platinum as the working and counter electrodes, and Ag/AgCl as the reference electrode. The scan rate was 50 mV s^{-1}.

2.2. Synthesis

2.2.1. *N,N′-bis(2′-hydroxyethyl)-1,6,7,12-tetra-p-t-butylphenoxy-3,4,9,10-perylene tetracarboxylic diimide*

5

To a solution of 1,6,7,12-tetra-*p*-*t*-butylphenoxy-3,4,9,10-perylene tetracarboxylic dianhydride **4** (788 mg, 0.8 mmol) in toluene (50 ml) was added ethanolamine (488 mg, 4 mmol). The reaction mixture was heated under nitrogen atmosphere and refluxed for 20 h, cooled to 50 °C, petroleum ether (200 ml) was added into the reaction mixture till no more dark violet grain was precipitated, then filtered and washed with petroleum ether to gain the crude product, which was purified by column chromatography on silica gel (CH_2Cl_2/ethyl acetate, 15:1, v/v) to give the PDI **5** as red-brown solid. (628 mg, 75% yield). mp > 300 °C; δ_H ($CDCl_3$, 500 MHz) 8.15(4H, s), 7.12(8H, d, *J* 8.45 Hz), 6.75(8H, d, *J* 8.36 Hz), 4.32(4H, t, *J* 6.93 Hz), 3.85(4H, m, *J* 6.65 Hz), 1.20(36H, s); Found: C, 76.05, H 6.13, N 2.50. $C_{68}H_{66}N_2O_{10}$ requires C, 76.24, H 6.21, N 2.61%; *m/z* (ESI^+): 1093.5(M^++Na).

2.2.2. *N,N′-bis(4′-aminophenyl)-1,6,7,12-tetra-p-t-butylphenoxy-3,4,9,10-perylene tetracarboxylic diimide*

6

1,6,7,12-tetra-*p*-*t*-butylphenoxy-3,4,9,10-perylene tetracarboxylic dianhydride **4** (394 mg, 0.4 mmol), 1,4-phenylenediamine (648 mg, 6 mmol) and imidazole (2.00 g, 31.2 mmol) were added to 180 ml of dried fresh distilled pyridine and brought to reflux under nitrogen atmosphere for 15 h, cooled. 500 ml of water was added to the reaction mixture and violet fine solid was precipitated, filtered and washed with water to gain the crude product, which was purified by column chromatography on silica gel (CH_2Cl_2/ethyl acetate, 25:1, v/v) to afford the PDI **6** as violet solid (342 mg, 68% yield). mp > 300 °C; δ_H ($CDCl_3$, 500 MHz) 8.16(4H, s), 7.13–7.17(16H, m), 6.77(8H, d, *J* 8.37 Hz), 1.20(36H, s); Found: C, 78.08, H 5.80, N 4.77. $C_{76}H_{68}N_4O_8$ requires C, 78.33, H 5.88, N 4.81%; *m/z* (ESI^+): 1165.4(M^++1).

2.2.3. *TTF-CO_2Et* ***9***

TTF-mono-CH_2CH_2CN **8** (1.134 g, 2 mmol) was dissolved in dried DMF (80 ml) and degassed with N_2 for 30 min. A solution of $CsOH{\cdot}H_2O$ (0.336 mg, 2.10 mmol) in dry MeOH (10 ml) was added dropwise to the mixture over a period of 15 min. After stirring for another 30 min, excess ethyl bromoacetate (2.5 ml, 22 mmol) was added and the solution turned from dark-orange to yellow-orange. The reaction mixture was stirred for another 6 h. The solvent and excess ethyl bromoacetate were removed under reduced pressure and the residue was purified by column chromatography on silica

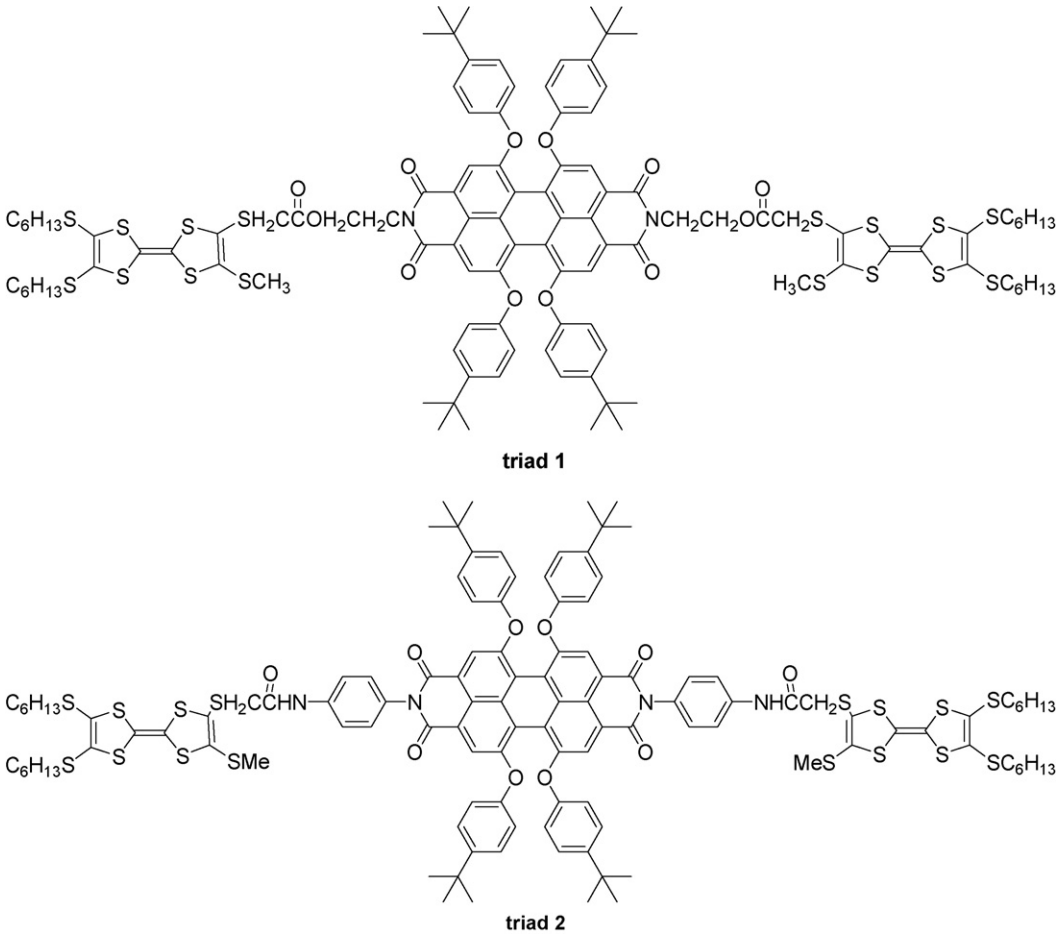

Fig. 2. The structures of triads **1** and **2**.

gel (CH_2Cl_2/petroleum ether, 1:3, v/v) to give the TTF-CO_2Et **9** as dark-orange oil. (950 mg, 79% yield). δ_H ($CDCl_3$, 500 MHz) 4.13(2H, t, *J* 7.11 Hz), 3.51(2H, s), 2.77(4H, br t), 2.36(3H, s), 1.60–1.68(4H, br m) 1.33–1.38(4H, m) 1.30–1.28(11H, m), 0.82 (6H, t, *J* 6.69 Hz); *m/z* (EI): 600.1(M^+, 100) 513.0(32) 482.0(12).

2.2.4. TTF-COOH **10**

A solution of LiOH·H_2O (269 mg, 6.4 mmol in 15.4 ml H_2O) was added to a stirred solution of TTF-CO_2Et **9** (769 mg, 1.3 mmol) in 1,4-dioxane (102 ml) at room temperature. After stirring for 20 h, HCl (5 M, 3.6 ml, 18.1 mmol) was added dropwise and the solution stirred for 15 min. Diethyl ether (100 ml) and water (13 ml) were added followed by adjusting pH with 5 M HCl to 1. The organic layer was isolated, dried over anhydrous $MgSO_4$ and the solvent was evaporated under reduced pressure. The dark brown solid was purified by column chromatography on silica gel (CH_2Cl_2/petroleum ether, 2:1, v/v, and then CH_2Cl_2/ethyl acetate, 1:1, v/v) to gain the TTF-COOH **10** as dark-orange solid (594 mg, 82% yield). mp 82–83 °C; δ_H ($CDCl_3$, 500 MHz) 3.80–4.00(2H, s br), 2.83(4H, t, *J* 6.92 Hz), 2.35–2.42(3H, t br), 1.84–1.90(4H, m) 1.55–1.58(4H, m) 1.18–1.24(8H, m), 0.81(6H, t, *J* 6.69 Hz); ν_{max} (KBr)/cm^{-1}: ν 2970, 1693, 1408, 1269, 1137; *m/z* (EI): 572.0(M^+, 100) 512.9(51) 528.0(24) 482.0(29).

2.2.5. Triad **1**

To a suspension of TTF-CO_2H **10** (114 mg, 0.2 mmol) in dried CH_2Cl_2 (8 ml) were added successively dicyclohexylcarbodiimide (45.2 mg, 0.22 mmol), 4-(dimethylamino)pyridine (24 mg,

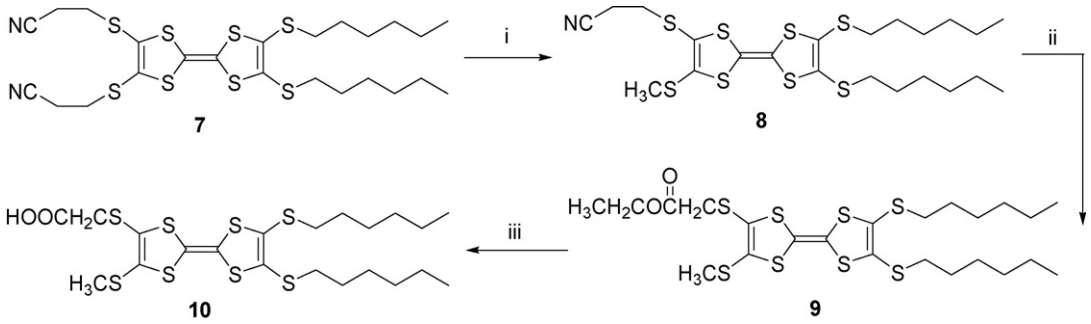

Scheme 3. Reagents and conditions: (i) DMF, CsOH·H_2O/methanol, MeI, RT, under N_2 atmosphere, 85%; (ii) DMF, CsOH·H_2O/methanol, $BrCH_2COOCH_2CH_3$, under N_2 atmosphere, 79%; (iii) 1,4-dioxane, LiOH·H_2O, RT 20 h, under N_2 atmosphere, 82%.

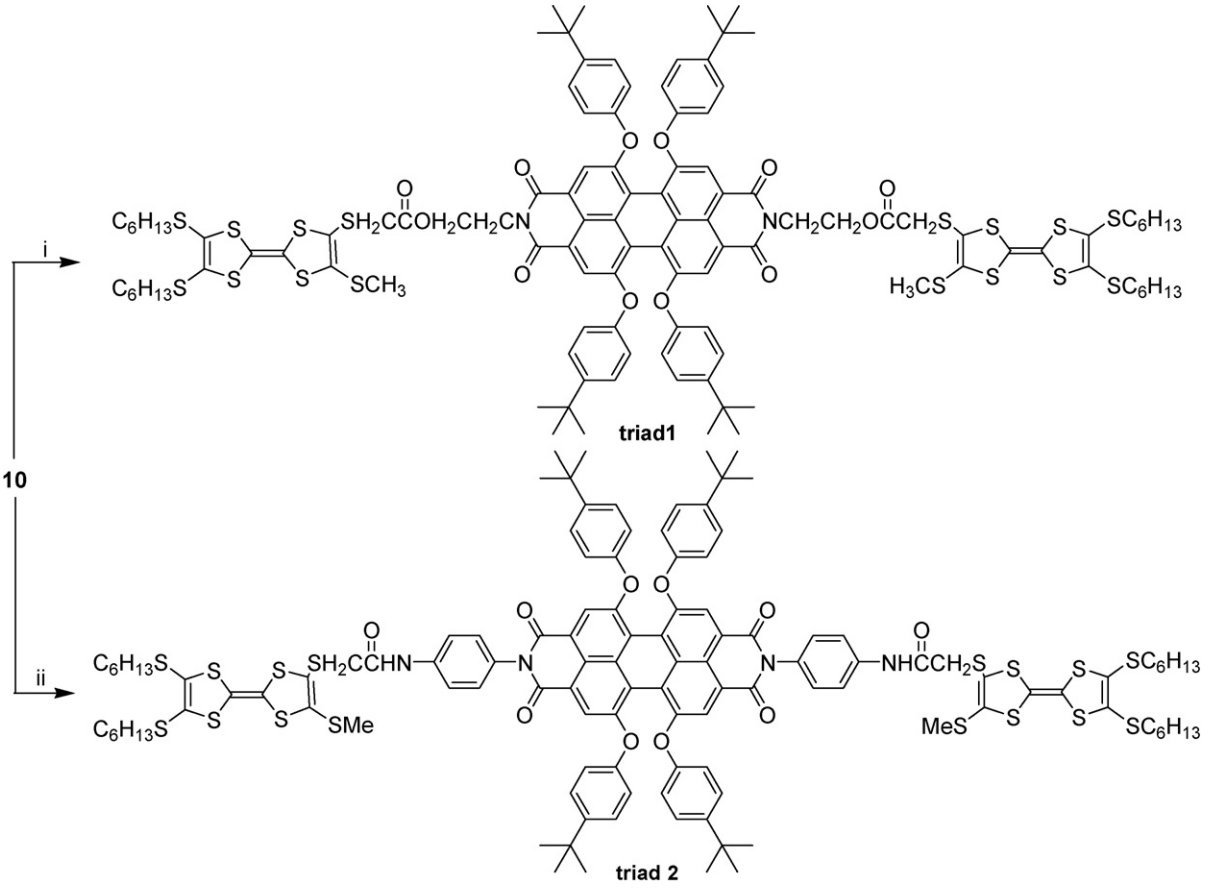

Scheme 4. Reagents and conditions: (i) PDI **5**, DCC, DMAP, HOBT, CH_2Cl_2, RT 48 h, under N_2 atmosphere, 78%; (ii) PDI **6**, DCC, DMAP, HOBT, pyridine, 80–90 °C, 72 h, under N_2 atmosphere, 55%.

0.2 mmol), 1-hydroxybenzotriazole (27 mg, 0.2 mmol) and PDI **5** (107 mg, 0.1 mmol) under nitrogen atmosphere. The reaction mixture was stirred at room temperature for 48 h. After removed the solvent under reduced pressure, the residue was purified by column chromatography on silica gel (CH_2Cl_2) and triad **1** was isolated as dark violet crystals. (169 mg, 78% yield) mp 244–245 °C; δ_H ($CDCl_3$, 500 MHz) 8.17(4H, s), 7.16 (8H, d, *J* 8.45 Hz), 6.76(8H, d, *J* 8.36 Hz), 4.40(8H, t, *J* 6.93 Hz), 3.39(4H, s), 2.73(8H, br t), 2.28(6H, s), 1.51–1.55(8H, m) 1.30–1.37(8H, m) 1.20–1.25(52H, m), 0.83(12H, t, *J* 5.30 Hz); δ_C ($CDCl_3$, 100 MHz) 168.7, 163.5, 155.9, 153.0, 147.3, 132.9, 127.8, 126.6, 122.1, 120.9, 120.3, 119.6, 119.3, 62.8, 38.9, 36.6, 34.4, 31.48, 29.8, 28.2, 22.5, 19.3, 14.03; Found: C, 60.01, H 5.78, N 1.19. $C_{110}H_{126}N_2S_{16}O_{12}$ requires C, 60.57, H 5.82, N 1.28%; *m/z* (ESI^+): 2201.8(M^++Na).

*2.2.6. Triad **2***

To a suspension of TTF-CO_2H **10** (228 mg, 0.4 mmol) in dried pyridine (30 ml) were added successively dicyclohexylcarbodiimide (91 mg, 0.44 mmol), 4-(dimethylamino)pyridine (48 mg, 0.4 mmol), 1-hydroxybenzotriazole (54 mg, 0.4 mmol) and then PDI **6** (232 mg, 0.2 mmol) under nitrogen atmosphere. The reaction mixture was stirred at 80–90 °C for 72 h, cooled. Water (100 ml) was added to the reaction mixture and dark violet solid was precipitated, filtered and washed with water to gain the crude product, which was purified by column chromatography on silica gel (CH_2Cl_2) and triad **2** was isolated as dark violet crystals. (249 mg, 55% yield) mp 243–244 °C; δ_H ($CDCl_3$, 500 MHz) 8.89–9.02 (2H, br s), 8.17(4H, s), 7.68(4H, d, *J* 8.62 Hz), 7.14(12H, d, *J* 8.38 Hz), 6.76(8H, d, *J* 8.40 Hz), 3.55–3.78(4H, br s), 2.75 (8H, br t, *J* 6.82 Hz), 2.32(6H, br s), 1.70–1.80(8H, m) 1.31–1.38(8H, m) 1.16–1.23(52H, m), 0.83(12H, t, *J* 5.56 Hz); δ_C ($CDCl_3$, 100 MHz) 165.1, 163.6, 156.1, 152.8, 147.4, 137.8, 135.0, 133.1, 131.2, 129.3, 128.0, 126.7, 122.5, 120.8, 120.0, 119.7, 119.3, 40.3, 38.0, 36.4, 34.4, 31.4, 31.3, 29.7, 28.2, 22.5, 19.7, 14.1; Found: C 61.98, H 5.64, N 2.33. $C_{118}H_{128}N_4S_{16}O_{10}$ requires C 62.29, H 5.67, N 2.46%; *m/z* (ESI^+): 2296.2(M^++Na).

3. Results and discussion

3.1. Synthesis

To obtain the triad **1** and triad **2**, *N*,*N*′-bis(2′-hydroxyethyl)-1,6,7,12-tetra-*p*-*t*-butylphenoxy-3,4,9,10-perylene tetracarboxylic diimide **5** (PDI **5**) and *N*,*N*′-bis(4′-aminophenyl)-1,6,7,12-tetra-*p*-*t*-butylphenoxy-3,4,9,10-perylene tetracarboxylic diimide **6** (PDI **6)** were used to react with TTF-CO_2H **10** for the synthetic strategy. The symmetrical PDI **5** and PDI **6** tetrasubstituted by *p*-*t*-butylphenoxy at the bay region were obtained efficiently by direct condensation of 2-aminoethanol and *p*-phenylenediamime with 1,6,7,12-tetra-*p*-*t*-butylphenoxy-3,4,9,10-perylene tetracarboxylic dianhydride **4** under nitrogen atmosphere, respectively (Scheme 2). The PDI **5** was afforded in 75% yield after silica gel column chromatography with toluene as reaction solvent, while the synthesis of PDI **6** was carried out in pyridine using imidazole as catalyst yielding 68%. The concentration of reactants should be much diluted and the *p*-phenylenediamime needed to excess largely in order to avoid forming the poly-PDI.

The monoacid TTF-CO_2H **10** was synthesized with gram-prepared TTF-bis-CH_2CH_2CN **7** as starting material (Scheme 3) [36–38]. TTF **7** was mono-deprotected using one equivalent of $CsOH{\cdot}H_2O$, subsequent alkylation with the MeI to give TTF **8** in

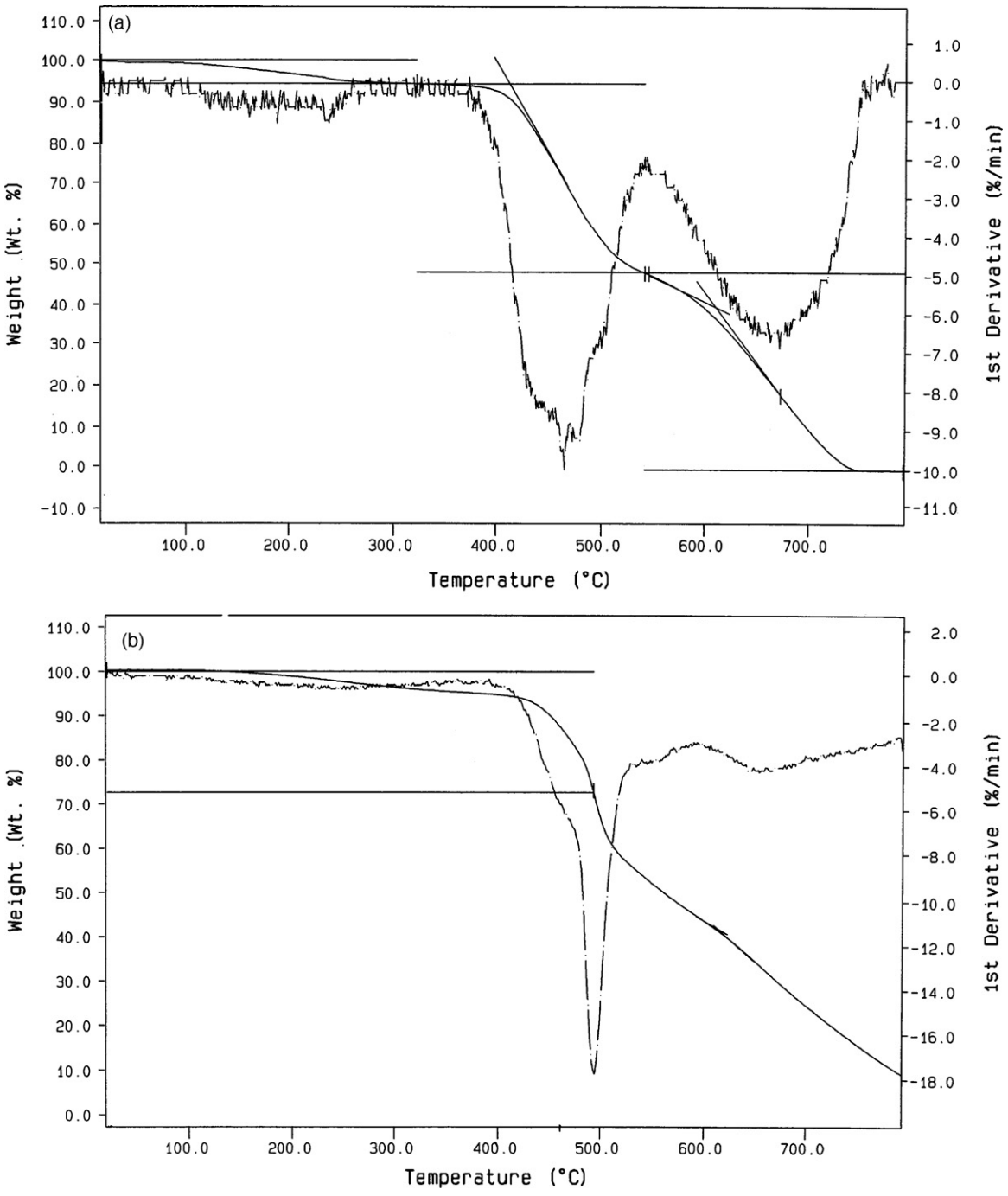

Fig. 3. Thermogravimetric analysis curves of PDI **5** and PDI **6** at a heating rate of 20 °C/min in oxygen.

85% yield. Then one equivalent of $CsOH{\cdot}H_2O$ was used to deprotect another cyanoethyl of TTF **8**, subsequent excess of ethyl bromoacetate was used as electrophile to form TTF **9**, yielding 79%. Hydrolysis of the ester group in TTF 9 gave the monoacid TTF-CO_2H **10** in 82% yields, according to reported procedures [39,40]. This three-step transformation of bis-cyanoethyl TTF **7** into the monoacid TTF **10** proved to offer the much easy-operating reactions with common organic reagents [41]. TTF **9** was chosen as the reference compound for further studies of triad **1** and triad **2**.

Esterification reaction between TTF **10** and PDI **5** using dicyclohexylcarbodiimide (DCC) as the coupling reagent together with 4-(dimethylamino)pyridine (DMAP) and 1-hydroxybenzotriazole (HOBT) afforded triad **1** [32], yielding 78%. With the similar reaction process, triad **2** was synthesized in 55% yields. As the reaction activity of aryl amine was much lower than the alkyl alcohol, the synthesis of triad **1** was carried out at room temperature with a shorter reaction time (48 h) while the synthesis of triad **2** was realized in pyridine at 80–90 °C with longer reaction time (72 h) and a lower yield.

3.2. Thermal stability of PDIs

Thermal analyses were studied by thermal gravimetric analysis (TGA) to prove the excellent thermal stability of the functional PDI **5** (Fig. 3a) and PDI **6** (Fig. 3b). The ΔH of these two compounds implied no melting points for them but the decomposition temper-

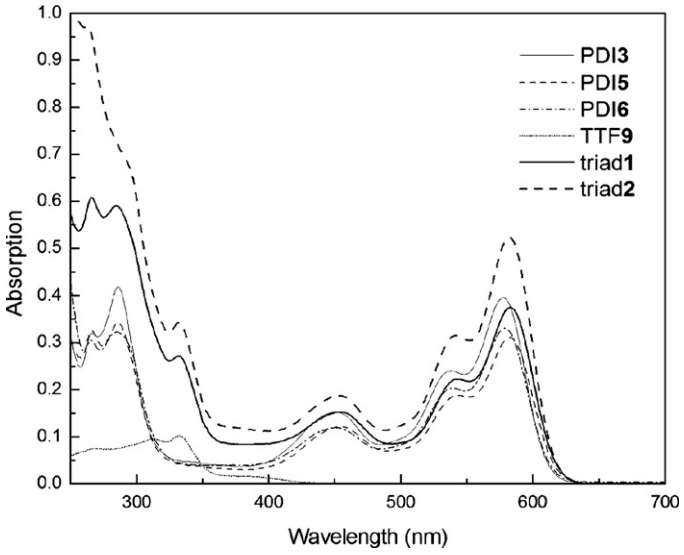

Fig. 4. The absorption spectra of PDI **3**, PDI **5**, PDI **6**, triads **1** and **2** in CH_2Cl_2, $c = 10^{-5}$ mol/L.

ature for both PDI **5** and **6**. The degradative temperature range of PDI **5** was 536–378 °C with a decomposition temperature of 412 °C, and the degradative temperature range of PDI **6** was 540–415 °C with a decomposition temperature of 453 °C, with a heating rate of 20 °C/min in oxygen. The results were coincident with former study [42] that the decomposition temperature *N*-aryl substituted PDI dye was higher than *N*-alkyl substituted PDI dye, indicating that the degradation of an aryl group occurred at a higher temperature and the thermal stability of PDI **6** was better.

3.3. Electronic absorption

The UV–visible spectra of PDIs and triads showed a wide absorption in the visible range between 300 nm and 700 nm (Fig. 4, Table 1). With tetrasubstitutions of *p-t*-butylphenoxy at the bay region, PDIs were highly soluble in normal organic solvents, such as CH_2Cl_2, $CHCl_3$, ethyl acetate, acetone, DMF, toluene, pyridine. The absorption curves of PDIs **3**, **5**, **6** were nearly identical. All of these absorption curves exhibited the absorption maximum centered in the small range of 578–583 nm, with characteristic absorptions of perylene core near 540 nm and 450 nm. It is notable that despite the colors of PDIs at solid state were different, their absorption spectra in the same solvent were similar to the reported results [42].

The absorption curves of the triad **1** and triad **2** exhibited not only the similar characteristic absorption of PDI moiety, but also a new absorption shoulder at 332 nm, which could attribute to the TTF moiety by comparison with the TTF **9** and PDIs. Neither a new intramolecular charge transfer band above 600 nm nor

Table 1
The UV–vis absorption and fluorescence maximum wavelengths

Compound	UV–vis[a] (nm)	FL[b] (nm)	ΔE_{0-0} (eV)
PDI **3**	578, 538, 451	610	2.09
PDI **5**	583, 543, 455	618	2.07
PDI **6**	579, 539, 451	613	2.10
TTF **9**	332	–	–
Triad **1**	583, 544, 453, 332	616	2.11
Triad **2**	582, 542, 451, 332	617	2.11

[a] UV–visible spectrum was obtained at a concentration of 10^{-5} mol/L in CH_2Cl_2.
[b] Fluorescence spectra in CH_2Cl_2, $\lambda_{exc} = 540$ nm, $c = 10^{-5}$ mol/L.

Table 2
Maximum absorption wavelengths λ_{max} (nm), molar extinction coefficients ε_{max} ($1\ mol^{-1}\ cm^{-1}$), fluorescence quantum yields Φ_f ($\lambda_{exc} = 540$ nm), radiative lifetimes τ_0 (ns) of PDI **3**, PDI **5**, PDI **6**, triads **1** and **2** in CH_2Cl_2

	λ_{max}	ε_{max}	Φ_f	τ_0
PDI **3**	578	39563	1	19.70
PDI **5**	583	31141	0.78	24.64
PDI **6**	579	33066	0.018	23.04
Triad **1**	583	37531	0.072	21.71
Triad **2**	582	52336	0.043	15.84

the intermolecular interaction between TTF and PDI units in the 300–500 nm range was observed in triad **1** and triad **2**. In our previous work, a TTF and PDI dyad, the TTF was directly attached to the bay region of PDI unit, which led to a totally different absorption curve and proved the internal charge transfer interaction taken place in the molecular system. Hence, it could conclude that the spatial separation of the electron donor and acceptor was the primary reason for the negligible charge transfer interaction in the ground state.

3.4. Steady-state fluorescence and fluorescence lifetimes

The maximum absorption wavelengths λ_{max} (nm, CH_2Cl_2), fluorescence quantum yields Φ_f, radiative lifetimes τ_0 (ns) of PDIs and two triads were listed in Table 2. The theoretical radiative lifetimes τ_0 were calculated according to the formula: $\tau_0 = 3.5 \times 10^8/\nu^2_{max}\varepsilon_{max}\Delta\nu_{1/2}$, where ν_{max} stands for the wavenumber in cm^{-1}, ε_{max} for the molar extinction coefficient at the selected absorption wavelength and $\Delta\nu_{1/2}$ indicated the half-width of the selected absorption in units of cm^{-1} [43].

The emission spectra of all the PDIs and triads were excited at $\lambda_{exc} = 540$ nm with PDI **3** as the reference, as shown in Fig. 5 (Table 1). By comparison with the fluorescence spectrum of PDI **3**, the fluorescence of PDI **5** was decayed in a slight degree while the fluorescence of PDI **6** was quenched thoroughly. It was not difficult to find out the structure differences between PDI **6** with other two PDIs. As *N*-aryl group is substituted with an electron donating group at para-position, the new molecular system would have a donor–acceptor–donor–acceptor–donor combination. So a photoinduced electron transfer (PET) interaction would happen in this molecule [2]. Another important evidence for this PET interaction

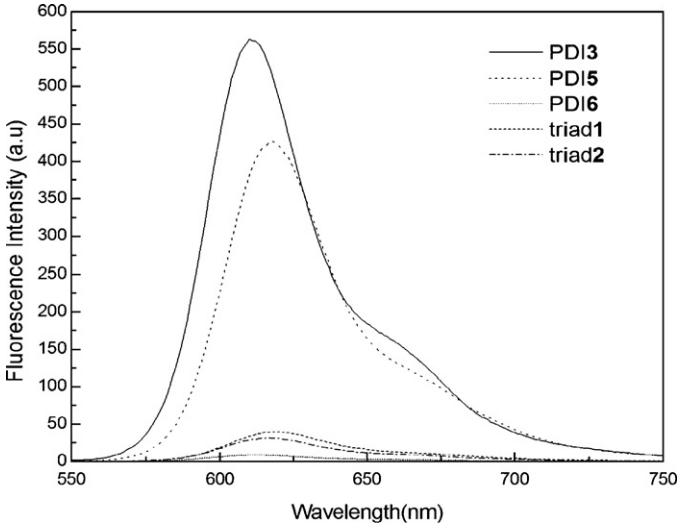

Fig. 5. The fluorescence spectra of PDI **3**, PDI **5**, PDI **6**, triads **1** and **2** in CH_2Cl_2, $\lambda_{exc} = 540$ nm, $c = 10^{-5}$ mol/L.

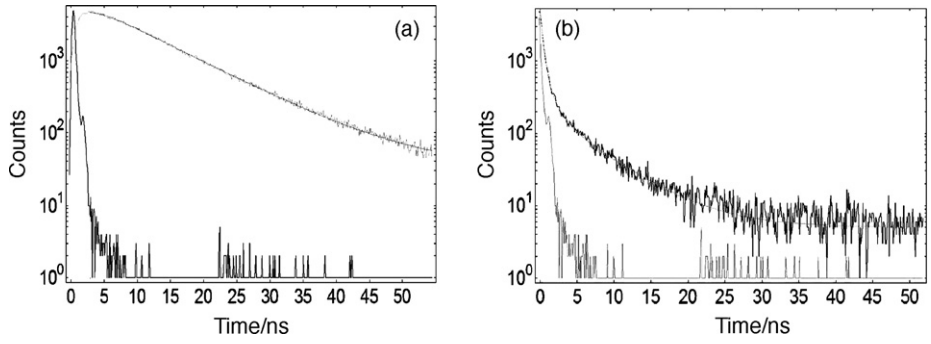

Fig. 6. The fluorescence decay curves of triad **1** (a) and triad **2** (b), in CH_2Cl_2, $c = 10^{-5}$ mol/L, $E_x = 440$ nm, $E_m = 616$ nm.

was provided by the electrochemical study of PDI **6** and a new oxidation potential was observed at 0.66v.

Without exception, the fluorescence intensities of triad **1** and triad **2** were quenched almost quantitative. This phenomenon could be ascribed to an intramolecular process due to two main reasons: (1) the PET process is thermodynamically favorable as the calculated free energy (ΔG_{PET}) is estimated to be −1.00 eV for triad **1** and triad **2** (calculated by the Rehm–Weller equation) [32,44,45]; (2) there was no spectral overlap of the absorption curve of TTF unit and the fluorescence curve of PDI unit, hence the energy transfer process from PDI* to TTF was prohibited according to the Förster mechanism [33].

The fluorescence quantum yields of PDIs were reduced because of the bis-substitution at the imide region. This result was in agreement with earlier comment [46], that the fluorescence quantum yield of perylene bis-substitution diimides was dominantly dependent on the type of the substitution. The low fluorescence quantum yield of PDI **6** indicated that perylene *p*-aniline diimide derivative could be used as at photo electron transfer reactions.

The fluorescence decay curves of triads **1**, **2** were shown in Fig. 6. The technique of time correlated single photon counting was used to record fluorescence lifetimes of the compounds, and measured fluorescence lifetimes were offered (Table 3). The calculated fluorescence lifetimes $\tau_f' = \tau_0 \Phi_f$ and the rate of fluorescence from $k_f = 1/\tau_f'$ were presented in Table 3 as comparison.

The fluorescence decays of PDI **3** and **5** could be well-fitted by the single-exponential decay component and the fluorescence lifetimes were 6.28 ns and 5.97 ns, respectively. The fluorescence decay curves of PDI **6**, triad **1** and **2** were double-exponential and analyzed by using the standard method of iterative reconvolution and non-linear least square fitting method. The fluorescence lifetimes of PDI **6**, triad **1** and **2** were consisted of a fast major component (the intramolecular interaction between donor and acceptor) and a decay minor component (PDI moiety). Take into account the facts that the strongly quench of the fluorescence in PDI **6**, triad **1** and **2** and the PET interaction might be the reason for this phenomenon, the photoinduced electron transfer from the donor counterpart to the PDI moiety could be the rate-determining step, followed by the fast charge recombination to the ground state. Comparing the fluorescence lifetimes of all the compounds, the reduced tendency of fluorescence lifetimes would be deduced, which was in good agreement with the fluorescence intensity reduction in CH_2Cl_2. As can be seen from Table 3, the calculated fluorescence lifetimes of all the compounds were in the same reduced tendency and similar to the measured fluorescence lifetimes.

Table 3
The measured fluorescence lifetimes τ_f (ns)[a], calculated fluorescence lifetimes τ_f' (ns) and fluorescence rate constants k_f (10^8 s^{-1})

Compounds	τ_f	τ_f'	k_f
PDI **3**	6.28 (100%)	19.70	0.5
PDI **5**	5.97 (100%)	19.20	0.5
PDI **6**	0.26 (62.79%), 6.05 (37.21%)	0.42	23
Triad **1**	1.72 (63.44%), 5.27 (36.56%)	1.56	6
Triad **2**	0.45 (62.40%), 6.01 (37.59%)	0.68	14

[a] The measured fluorescence lifetimes were obtained in CH_2Cl_2, $c = 10^{-5}$ mol/L, $E_{ex} = 440$ nm, $E_{em} = 616$ nm, corresponding to the emission maxima of the PDI chromophore in CH_2Cl_2.

3.5. Chemical oxidation

The fluorescence intensity of the PDI moiety was strongly quenched in triad **1** and **2**, so, if the TTF units of triad **1** and **2** could be oxidized chemically or electrochemically, the photoinduced electron-transfer from TTF to PDI units could be hindered. The fluorescence intensity of **1** and **2** could be increased. This approach has been wide applied in recent year for the construction of new molecular switches [28–31]. The chemical oxidation experiments were carried out to test the potential of the triad **1** and triad **2** as the fluorescence switches by adding excess of diacetoxyiodobenzene in the presence of triflic acid ($PhI(OAc)_2/CF_3SO_3H$) in CH_2Cl_2 (Fig. 7) [47]. The fluorescence emission was recorded without any supplementary addition of oxidation reagent. Consequently, the fluorescence intensity was gradually recovered at the TTF^{2+}–PDI–TTF^{2+} stage. The fluorescence intensity reached a limit value after about 120 min for triad **1** and 70 min for triad **2**, it implied that triad **2** was easier to be oxidated than triad **1**, who was more stable than **2** in the excited state, which was agreed with the fluorescence lifetime results. The values of oxidative fluorescence intensity of triad **1** and triad **2** corresponded to around 35% and 58% of the fluorescence intensity of PDI **3** recorded with the same experiment condition.

The reversible processes of triad **1** and triad **2** were studied with adding excess zinc power to the solution in order to reduce TTF^{2+}–PDI–TTF^{2+} into TTF^0–PDI–TTF^0, the fluorescence intensity of both triads was quenched again and the initial fluorescence spectra were almost completely recovered (Fig. 8). The chemical oxidation and reduction paths clearly indicated that triad **1** and triad **2** could be employed as the reversible fluorescence-redox switch with a good solubility in organic solvents.

3.6. Electrochemistry

The cyclic voltammetry (CV) data of all compounds (triad **1**, **2** PDI **3**, **5**, **6** and TTF 9) were given in Table 4. Both of triads had two wide one-electron reversible reduction position in the negative position, due to the successive formation of the radical anion TTF–$PDI^{\bullet -}$–TTF and dianion TTF–PDI^{2-}–TTF, respectively.

Two reversible TTF oxidation waves and one reversible PDI oxidation wave were shown in the positive direction, corresponding to the radical cation $TTF^{\bullet +}$–PDI–$TTF^{\bullet +}$, dication TTF^{2+}–PDI–TTF^{2+}

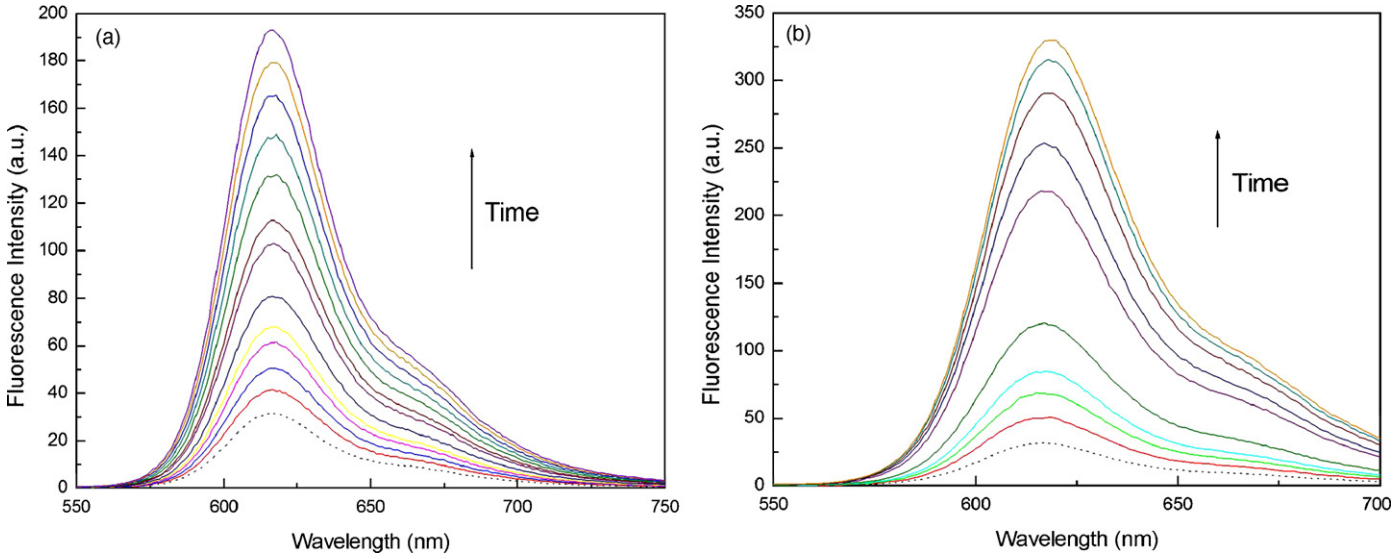

Fig. 7. Fluorescence emission spectra of triad **1** (a) and triad **2** (b) recorded before (dot line) and after addition of an excess of (diacetoxyiodo)benzene in the presence of triflic acid in CH_2Cl_2 ($c = 10^{-5}$ mol/L, $\lambda_{exc} = 540$ nm).

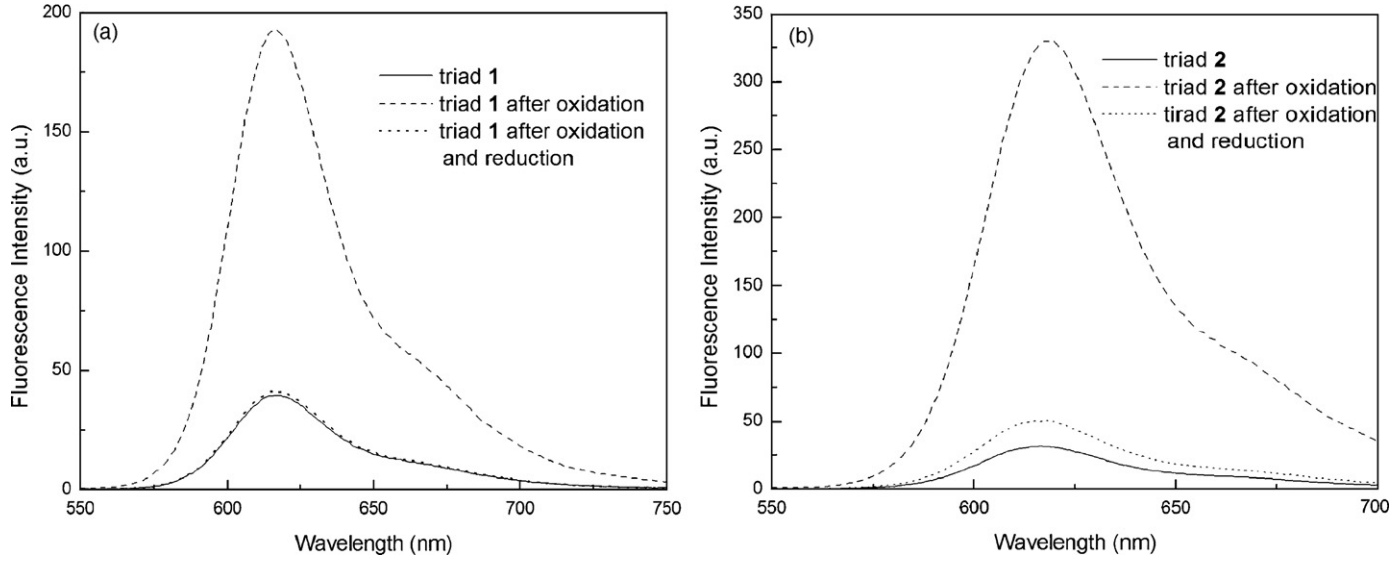

Fig. 8. Fluorescence emission spectra of triad 1 (a) and triad 2 (b), after oxidation and after oxidation and reduction paths (CH_2Cl_2, $c = 10^{-5}$ mol/L, $\lambda_{exc} = 540$ nm).

and TTF^{2+}–PDI^{+}–TTF^{2+}. The oxidation of PDI moiety was observed in the TTF–PDI donor–acceptor molecular systems in CH_2Cl_2 containing 0.1 M n-Bu_4NPF_6. Since the perylene moiety and the TTF moiety in triad **1** triad **2** showed their individual electrochemical characteristics, it indicated that neither intramolecular nor intermolecular interaction took place between both electroactive moieties in the ground state and the result was matched that of the UV/vis absorption. The HOMO orbital energies were calculated as $HOMO_{triad\ 1} = -5.68$ eV and $HOMO_{triad\ 2} = -5.66$ eV from cyclic voltammograms based on the value of 4.8 eV for Fc. Thus, the LUMO orbital energies were obtained as $LUMO_{triad\ 1} = -3.71$ eV and $LUMO_{triad\ 2} = -3.69$ eV with the equation $\Delta E_g(eV) = 1240/\lambda_{(nm)}$. The energetically minimized conformations of triad **1** (Fig. 9a) and triad **2** (Fig. 9b) were calculated with Gaussian(R) 03 program [48]. It is notable that two TTF groups were exposed, which benefited for them to take parts in redox processes [49].

Table 4
Electrochemical Data for triad **1**, triad **2**, PDI **3**, PDI **5**, PDI **6** and TTF **9** in CH_2Cl_2

Compound	$E_{1/2\ red2}$ [a,b]	$E_{1/2red1}$ [a,b]	$E_{1/2ox1}$ [a,b]	$E_{1/2ox2}$ [a,b]	$E_{1/2ox3}$ [a,b]
Triad **1**	−0.88	−0.59	0.62	0.96	1.39
Triad **2**	−0.87	−0.60	0.61	0.94	1.40
PDI **3**	−0.91	−0.60	–	–	1.37
PDI **5**	−1.03	−0.59	–	–	1.40
PDI **6**	−1.29	−0.60	0.66	–	1.41
TTF **9**	–	–	0.61	0.94	–

[a] The values (V) were recorded in CH_2Cl_2 solution using nBu$_4$NPF$_6$ 0.1 M in CH_2Cl_2 as supporting electrolyte, AgCl/Ag as the reference electrodes, platinum wires as counter and working electrodes, scan rate: 50 mV/s.

[b] versus AgCl/Ag.

The first reduction potentials of perylene units for all the compounds were nearly identical (Table 4) and the corresponding potentials of the radical anion were around −0.60 V. The second reduction potentials of perylene units were shifted, according to pervious study [42], the difference on this reduction step was attributed to the substituents effects at the imide region. The oxida-

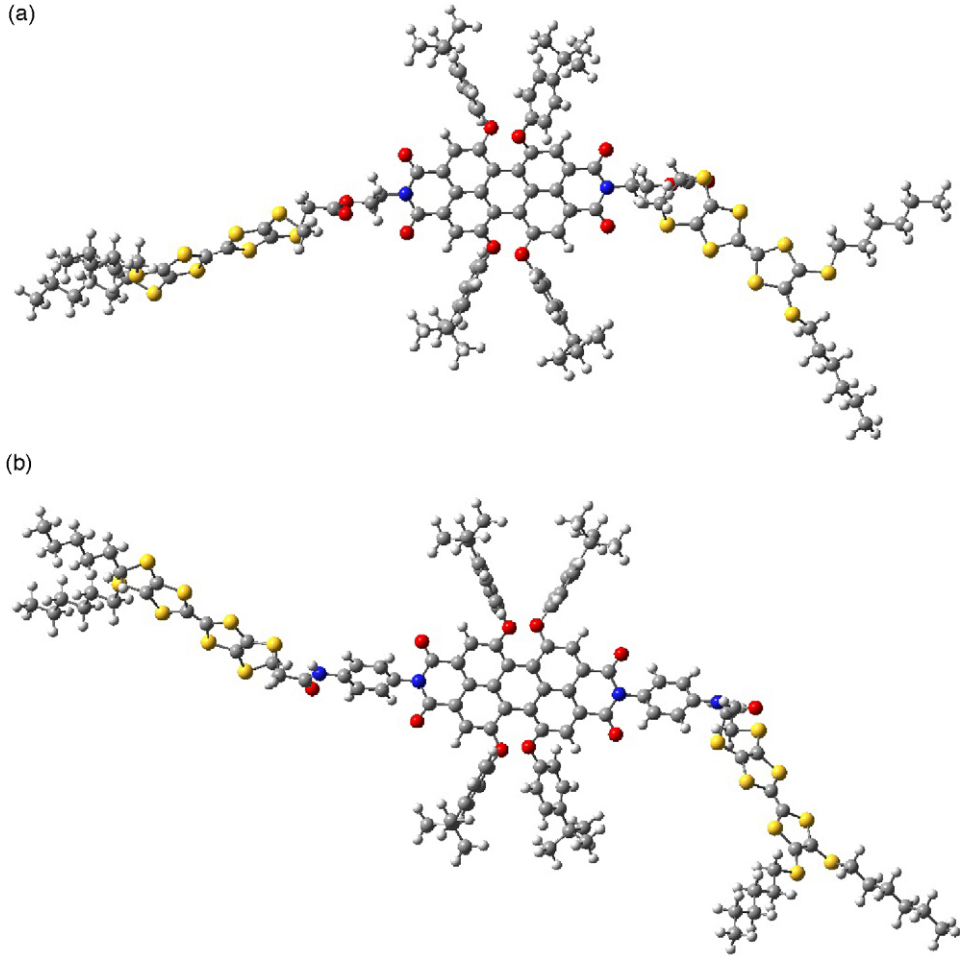

Fig. 9. Energetically minimized structures of triad **1** (a) and triad **2** (b), modeled using Gaussian(R) 03 program, gray = carbon; white = hydrogen; red = oxygen; blue = nitrogen; yellow = sulfur.

tion potentials of PDIs became much lower than the unsubstituted PDIs (+2.32 V to +2.85 V, respectively [32]), indicating that tetrasubstituted *p*-*t*-butylphenoxy at the "bay" region made the perylene compounds much easier to be oxidated. It could be due to the substitutions made the perylene framework twisted and the electron could be lost easily as the descent strength of delocalization pathway for the 20 π-electron system. The energetically minimized conformations of PDI **5** (Fig. 10a) and PDI **6** (Fig. 10b) were offered

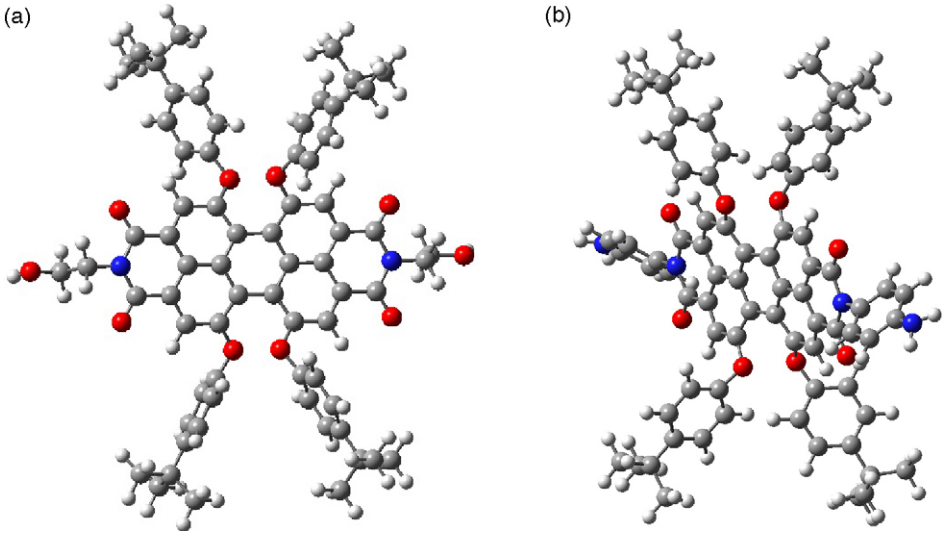

Fig. 10. Energetically minimized structures of PDI **5** (a) and PDI **6** (b), modeled using Gaussian(R) 03 program, gray = carbon; white = hydrogen; red = oxygen; blue = nitrogen.

with Gaussian(R) 03 program [50], the twisted structure of perylene framework was obtained because of the electrostatic repulsion and steric effect among these four aryl substitutions.

4. Conclusions

Several highly soluble perylene compounds (PDI **3**, PDI **5** and PDI **6**) were synthesized as well as TTF compounds (TTF **9** and TTF **10**). Two donor–acceptor–donor molecular systems, triads **1**, **2**, were afforded by combining PDIs and TTFs compounds. The solubility of PDIs was enhanced greatly because of tetra-substituted *p*-*t*-butylphenoxy at the bay region, while the thermal stability remained, which made these PDIs useful in material science. The VU/vis absorption spectra of PDIs implied that the substituents are not involved in the chromophore. The absorption spectra of triads in solution were the addition of PDI and TTF units, indicating no intramolecular charge transfer interaction for triad **1**, **2** in their ground state. The fluorescence spectra implied that the type of the substitution of perylene bis-substitution diimides played an important role in the fluorescence behavior. The PET interaction was proved in the triad **1**, triad **2** and PDI **6** by the fluorescence spectra and theoretical calculation. Differences between the second reduction potentials of PDIs were observed. The redox potentials of the triads exhibited no shift compared to the individual PDI and TTF also indicating no internal charge transfer interaction occurred in triad **1**, **2** in their ground state. The chemical oxidation experiments indicated the fluorescence intensity was depending on the oxidation state of TTF unit in triad **1**, **2**, which could be considered as new kinds of fluorescence redox molecular switches with reasonable big molecular weight, good solubility.

Acknowledgements

This work was supported by National Natural Science Foundation of China (No. 20676036) and the Key Project of the Ministry of Education of China (No. 03053).

References

[1] H. Icil, E. Arslan, Synthesis and spectroscopic properties of highly pure perylene fluorescent dyes, Spectrosc. Lett. 34 (2001) 355–363.
[2] H. Icil, S. Icli, The synthesis and spectral characteristics of a supramolecular model: perylene 3,4,9,10-tetracarcoxylic acid-*bis*-*N*,*N*′-*p*-aminophenyl diimide, Spectrosc. Lett. 28 (1995) 595–601.
[3] H. Icil, D. Uzun, E. Arslan, Synthesis and spectroscopic characterization of water soluble perylene tetracarboxylic diimide derivatives, Spectrosc. Lett. 34 (2001) 605–614.
[4] J.M. Serin, D.W. Brousmiche, J.M.J. Fréchet, Cascade energy transfer in a conformationally mobile multichromophoric dendrimer, Chem. Commun. (2002) 2605–2607.
[5] U. Rohr, C. Kohl, K. Müllen, A. Craats, J. Warman, Liquid crystalline coronene derivatives, J. Mater. Chem. 11 (2001) 1789–1799.
[6] K. Kohl, Highly fluorescent and water-soluble perylene dyes, Chem. Eur. J. 10 (2004) 5297–5310.
[7] V.J. Sapagovas, V. Gaidelis, V. Kovalevskij, A. Undzenas, 3,4,9,10-Perylenetetracarboxylic acid derivatives and their photophysical properties, Dyes Pigments 71 (2006) 178–187.
[8] Y. Nagao, T. Naito, Y. Abe, T. Misono, Synthesis and properties of long and branched alkyl chain substituted perylenetetracarboxylic monoanhydride monoimides, Dyes Pigments 32 (1996) 71–83.
[9] S. Icli, H. Icil, A thermal and photostable reference probe for Q_f measurements: chloroform soluble perylene 3,4,9,10-tetracarboxylic acid-bis-*N*,*N*′-dodecyl diimide, Spectrosc. Lett. 29 (1996) 1253–1257.
[10] J.L. Segura, R. Gómez, E. Reinold, P. Bauerle, Synthesis and electropolymerization of a perylenebisimide-functionalized 3,4-ethylenedioxythiophene (EDOT) derivative, Org. Lett. 7 (2005) 2345–2348.
[11] R. Gómez, J.L. Segura, N. Martin, Highly efficient light-harvesting organofullerenes, Org. Lett. 7 (2005) 717–720.
[12] P. Schlichting, U. Rohr, K. Müllen, New synthetic routes to alkyl-substituted and functionalized perylenes, Liebigs. Ann. (1997) 395–407.
[13] C. Ego, D. Marsitzky, S. Becker, J.Y. Zhang, A.C. Grimsdale, K. Müllen, J.D. MacKenzie, C. Silva, R.H. Firend, Attaching perylene dyes to polyfluorene: three simple, efficient methods for facile color tuning of light-emitting polymers, J. Am. Chem. Soc. 125 (2003) 437–443.
[14] S. Leroy-Lhez, L. Perrin, J. Baffreau, P. Hudhomme, Perylenediimide derivatives in new donor–acceptor dyads, C. R. Chim. 9 (2006) 240–246.
[15] J. Baffreau, L. Perrin, S. Leroy-Lhez, P. Hudhomme, Perylene-3,4:9.10-bis(dicarboximide) linked to [60]fullerene as a light-harvesting antenna, Tetrahedron Lett. 46 (2005) 4599–4603.
[16] C.C. Chao, M. Leung, Y.O. Su, K.Y. Chiu, T.H. Lin, S.J. Shieh, S.C. Lin, Photophysical and electrochemical properties of 1,7-diaryl-substituted perylene diimides, J. Org. Chem. 70 (2005) 4323–4331.
[17] F. Würthner, Perylene bisimide dyes as versatile building block for functional supramolecular architectures, Chem. Commun. (2004) 1564–1579.
[18] R. Gómez, C. Coya, J.L. Segura, Synthesis of a π-extended TTF-perylenediimide donor–acceptor dyad, Tetrahedron Lett. 48 (2008) 3225–3228.
[19] C.C. You, C.R. Saha-Möller, F. Würthner, Synthesis and electropolymerization of novel oligothiophene-functionalized perylene bisimides, Chem. Commun. (2004) 2030–2031.
[20] M.P. O'Neil, M.P. Niemczyk, W.A. Svec, D. Gosztola, G.L. Gaines, M.R. Wasielewski, Picosecond optical switching based on biphotonic excitation of an electron donor–acceptor–donor molecular, Science 257 (1992) 63–65.
[21] M.O. Liu, C.H. Tai, A.T. Hu, The fluorescent and photoelectric conversion properties of phthalocyanine–perylene tetracarboxylic complexes, J. Photochem. Photobiol. A: Chem. 165 (2004) 193–200.
[22] P. Bauer, H. Wietasch, S.M. Lindner, M. Thelakkat, Synthesis and characterization of donor-bridge-acceptor molecular containing tetraphenylbenzidine and perylene bisimide, Chem. Mater. 19 (2007) 88–94.
[23] J.L. Segura, N. Martin, New concepts in tetrathiafulvalene chemistry, Angew. Chem. Int. Ed. 40 (2001) 1372–1409.
[24] C.A. Christensen, A.S. Batsanov, M.R. Bryce, Thiolated π-extended tetrathiafulvalenes: versatile multifunctional π-systems, J. Org. Chem. 72 (2007) 1301–1308.
[25] C.A. Christensen, A.S. Batsanov, M.R. Bryce, Extreme conformational constraints in π-extended tetrathiafulvalenes: unusual topologies and redox behavior of doubly and triply birdged cyclophanes, J. Am. Chem. Soc. 128 (2006) 10484–10490.
[26] M.R. Bryce, Tetrathiafulvalenes as π-electron donors for intarmolecular charge-transfer materials, Adv. Mater. 11 (1999) 11–23.
[27] J.O. Jeppesen, J. Perkins, J. Becher, J.F. Stoddart, Slow shutting in an amphiphilic bistable [2]roxane incorporating a tetrathiafulvalene unit, Angew. Chem. Int. Ed. 40 (2001) 1216–1221.
[28] Z. Wang, D.Q. Zhang, D.B. Zhu, A new saccharide sensor based on a tetrathiafulvalene-anthracene dyad with a boronic acid group, J. Org. Chem. 70 (2005) 5729–5732.
[29] G.X. Zhang, D.Q. Zhang, X.F. Guo, D.B. Zhu, A new redox-fluorescence switch based on a triad with tetrathiafulvalene and anthracene units, Org. Lett. 6 (2004) 1209–1212.
[30] H.C. Li, J.O. Jeppesen, E. Levillain, J. Becher, A mono-TTF-annulated porphyrin as a Fluorescence switch, Chem. Commun. (2003) 846–847.
[31] C. Farren, C.A. Christensen, S. FitzGerlad, M.R. Bryce, A. Beeby, Synthesis of novel phthalocyanine–tetrathiafulvalene hybrids; intramolecular fluorescence quenching related to molecular geometry, J. Org. Chem. 67 (2002) 9130–9139.
[32] A fluorescence-redox switch is obtained if an oxidation/reduction of a switch molecular is combined with a photon read-out process. S. Leroy-Lhez, J. Baffreau, L. Perrin, E. Levillain, M. Allain, M-J. Blesa, P. Hudhomme, Tetrathiafulvalene in a perylene-3,4:9,10-bis(dicarboximide)-based dyad: a new reversible fluorescence-redox dependent molecular system, J. Org. Chem. 70 (2005) 6313–6320.
[33] X.F. Guo, D.Q. Zhang, H.J. Zhang, Q.H. Fan, W. Xu, X.C. Ai, L.Z. Fan, D.B. Zhu, Donor–acceptor–donor triads incorporating tetrathiafulvalene and perylene diimide units: synthesis, electrochemical and spectroscopic studies, Tetrahedron 59 (2003) 4843–4850.
[34] F. Würthner, C. Thalacker, A. Sautter, W. Schärtl, W. Lbach, O. Hollricher, Hierarchical self-organization of perylene bisimide-melamine assemblies to fluorescent mesoscopic superstructures, Chem. Eur. J. 6 (2000) 3871–3886.
[35] H. Kaiser, J. Lindner, H. Langhals, Synthese von nichtsymmetrisch substituierten Perylen-Fluoreszenzfarbstoffen, Chem. Ber. 124 (1991) 529–535.
[36] K.B. Simonsen, N. Svenstrup, J. Lau, O. Simonsen, P. MΦrk, G.J. Kristensen, J. Becher, Sequential functionalisation of bis-protected tetrathiafulvalene-dithiolates, Synthesis 3 (1996) 407–418.
[37] C.A. Christensen, M.R. Bryce, J. Becher, New multi(tetrathiafulvalene) dendrimers, Synthesis 12 (2000) 1695–1704.
[38] N. Svenstrup, K.M. Rasmussen, T.K. Hansen, J. Becher, The chemistry of TTFTT; 1: new efficient synthesis and reactions of tetrathiafulvalene-2,3,6,7-tetrathiolate (TTFTT): an important building block in TTF-syntheses, Synthesis 8 (1994) 809–812.
[39] R.P. Parg, J.D. Kilburn, M.C. Petty, C. Pearson, T.G. Ryan, A semiconducting langmuir-blodgett film of a non-amphiphilic bis-tetrathiafulvalene derivative, J. Mater. Chem. 5 (1995) 1609–1616.
[40] K. Heuzé, M. Fourmigué, P. Batail, The crystal chemistry of amide-functionalized ethylenedithiotetrathiafulvalenes: EDT-TTF-CONRR′ (R, R′ = H, Me), J. Mater. Chem. 9 (1999) 2373–2379.
[41] T. Devic, N. Avarvari, P. Batail, A series of redox active, tetrathiafulvalene-based amidopyridines and bipyridines ligands: syntheses, crystal structures, a radical cation salt and group 10 transition-metal complexes, Chem. Eur. J. 10 (2004) 3697–3707.

[42] N. Pasaogullari, H. Icil, M. Demuth, Symmetrical and unsymmetrical perylene diimides: their synthesis, photophysical and electrochemical properties, Dyes Pigments 69 (2006) 118–127.
[43] H. Langhals, L. Feiler, Pyrroli and thiophenoperylenedicarboximides highly fluorescent heterocycles, Liebigs. Ann. (1996) 1587–1591.
[44] D. Rehm, A. Weller, Irs. J. Chem. 8 (1970) 259–265, For tirad **1**: $\Delta G_{PET} = E_{(ox)} - E_{(red)} - E^{0-0}$(tirad **1**) $- \Delta e$, with $E_{(ox)} = +0.62$ eV, $E_{(red)} = -0.59$ eV, E^{0-0}(tirad **1**) = 2.11 eV, $\Delta e \approx 0.1$ eV; For tirad **2**: $E_{(ox)} = +0.60$ eV, $E_{(red)} = -0.61$ eV, E^{0-0}(tirad **2**) = 2.11 eV, $\Delta e \approx 0.1$ eV.
[45] Y. Shibano, T. Umeyama, Y. Matano, N.V. Tkachenko, H. Lemmetyinen, Y. Araki, O. Ito, H. Imahori, Large reorganization energy of pyrrolidine-substituted perylenediimide in electron transfer, J. Phys. Chem. C 111 (2007) 6133–6142.
[46] H. Langhals, Synthese von hochreinen Perylen-Fluoreszenzfarbstoffen in großen Mengen—gezielte Darstellung von Atrop-Isomeren, Chem. Ber. 118 (1985) 4621–4623.
[47] M. Giffard, G. Mabon, E. Leclair, N. Mercier, M. Allain, A. Gorgues, P. Molinié, O. Neilands, P. Krief, V. Khodorkovsky, Oxidation of TTF derivatives using (diacetoxyiodo)benzene: a general chemical route toward cation radicals, dications, and nonstoichiometric salts, J. Am. Chem. Soc. 123 (2001) 3852–3853.
[48] Structural optimization, using the standard procedure for energy minimization with Gaussian(R) 03 program, indicates that the most stable conformations for triads **1** and **2** are extended ones. The distance between the two ions was estimated by geometrical optimization using semiempirical AM 1 method as follows: 8 Å for triad **1** and 10 Å for triad **2**. Gaussian 03, Revision D.01, M.J. Frisch, G.W. Trucks, H.B. Schlegel, G.E. Scuseria, M.A. Robb, J.R. Cheeseman, J.A. Montgomery, Jr., T. Vreven, K.N. Kudin, J.C. Burant, J.M. Millam, S.S. Iyengar, J. Tomasi, V. Barone, B. Mennucci, M. Cossi, G. Scalmani, N. Rega, G.A. Petersson, H. Nakatsuji, M. Hada, M. Ehara, K. Toyota, R. Fukuda, J. Hasegawa, M. Ishida, T. Nakajima, Y. Honda, O. Kitao, H. Nakai, M. Klene, X. Li, J.E. Knox, H.P. Hratchian, J.B. Cross, V. Bakken, C. Adamo, J. Jaramillo, R. Gomperts, R.E. Stratmann, O. Yazyev, A.J. Austin, R. Cammi, C. Pomelli, J.W. Ochterski, P.Y. Ayala, K. Morokuma, G.A. Voth, P. Salvador, J.J. Dannenberg, V.G. Zakrzewski, S. Dapprich, A.D. Daniels, M.C. Strain, O. Farkas, D.K. Malick, A.D. Rabuck, K. Raghavachari, J.B. Foresman, J.V. Ortiz, Q. Cui, A.G. Baboul, S. Clifford, J. Cioslowski, B.B. Stefanov, G. Liu, A. Liashenko, P. Piskorz, I. Komaromi, R.L. Martin, D.J. Fox, T. Keith, M.A. Al-Laham, C.Y. Peng, A. Nanayakkara, M. Challacombe, P.M.W. Gill, B. Johnson, W. Chen, M.W. Wong, C. Gonzalez, J.A. Pople, Gaussian, Inc., Wallingford, CT, 2004.
[49] M.R. Bryce, W. Devonport, L.M. Goldenberg, C. Wang, Macromolecular tetrathiafulvalene chemistry, Chem. Commun. (1998) 945–951.
[50] Structural optimization, using the standard procedure for energy minimization with Gaussian(R) 03 program, implied that the four substitutions at the bay region twisting the perylene framework because of the electrostatic repulsion and steric effects. Gaussian 03, Revision D.01, M.J. Frisch, G.W. Trucks, H.B. Schlegel, G.E. Scuseria, M.A. Robb, J.R. Cheeseman, J.A. Montgomery, Jr., T. Vreven, K.N. Kudin, J.C. Burant, J.M. Millam, S.S. Iyengar, J. Tomasi, V. Barone, B. Mennucci, M. Cossi, G. Scalmani, N. Rega, G.A. Petersson, H. Nakatsuji, M. Hada, M. Ehara, K. Toyota, R. Fukuda, J. Hasegawa, M. Ishida, T. Nakajima, Y. Honda, O. Kitao, H. Nakai, M. Klene, X. Li, J.E. Knox, H.P. Hratchian, J.B. Cross, V. Bakken, C. Adamo, J. Jaramillo, R. Gomperts, R.E. Stratmann, O. Yazyev, A.J. Austin, R. Cammi, C. Pomelli, J.W. Ochterski, P.Y. Ayala, K. Morokuma, G.A. Voth, P. Salvador, J.J. Dannenberg, V.G. Zakrzewski, S. Dapprich, A.D. Daniels, M.C. Strain, O. Farkas, D.K. Malick, A.D. Rabuck, K. Raghavachari, J.B. Foresman, J.V. Ortiz, Q. Cui, A.G. Baboul, S. Clifford, J. Cioslowski, B.B. Stefanov, G. Liu, A. Liashenko, P. Piskorz, I. Komaromi, R.L. Martin, D.J. Fox, T. Keith, M.A. Al-Laham, C.Y. Peng, A. Nanayakkara, M. Challacombe, P.M.W. Gill, B. Johnson, W. Chen, M.W. Wong, C. Gonzalez, J.A. Pople, Gaussian, Inc., Wallingford, CT, 2004.